Supplemental Figure Legends:

Supplemental Fig. 1. EM of detergent solubilized intact $\alpha_{IIb}\beta_3$. Representative EM field views and all EM class averages of negatively stained DDM-solubilized $\alpha_{IIb}\beta_3$ in (A) Ca^{2+}/Mg^{2+}, (B) Mn^{2+}/Ca^{2+}, and (C) Mn^{2+}/Ca^{2+} and L-739758. Each box has a dimension of 100x100 pixels with 4.48 Å/pixel. The number of particles in each class average is denoted in each box.

Supplemental Fig. 2. Cross-correlation of EM class averages with atomic models. Representative class averages of $\alpha_{IIb}\beta_3$ in the (A) bent conformation from Ca^{2+}/Mg^{2+} and Mn^{2+}/Ca^{2+} conditions, (B) extended-closed conformation from Mn^{2+}/Ca^{2+} and Mn^{2+}/Ca^{2+} with L-739758, and (C) extended-open conformation from Mn^{2+}/Ca^{2+} and Mn^{2+}/Ca^{2+} with L-739758. The masked region used for cross-correlation calculations is shown below the respective class average. The atomic model used for each cross-correlation analysis is shown to the left. The cross-correlation coefficients for the best orientation with each model are denoted in the box of each respective back projection.

Supplemental Fig. 3. Atomic models of $\alpha_{IIb}\beta_3$. Atomic models of $\alpha_{IIb}\beta_3$ with modeled transmembrane domains in the (A) resting, bent conformation, (B) extended-closed conformation, (C) extended-open conformation based upon the full ectodomain crystal structure (PDB ID: 3FCS (8)) and EM class averages. The α_{IIb} subunit is colored in *red* and β_3 subunit in *blue*.

Supplemental Fig. 4. Distance distribution curves of $\alpha_{IIb}\beta_3$ atomic models. (A) Distance distribution curves generated from various atomic models. The bent model in *dark blue* is based on PBD ID: 3FCS. The extended-closed models are based upon β-knee orientations from PDB ID: 2P26 in *red*, PDB ID: 2P28 in *cyan*, and a fully extended conformation in *purple*. The extended-open models are based upon β-knee orientations from PDB ID: 2P26 in *pink*, PDB ID: 2P28 in *orange* and a fully extended conformation in *green*. (B-D) Comparison of distance distribution curves calculated from experimentally collected X-ray solution scattering curves (*black lines*) with the closest distance distribution curve from atomic models (*colored lines*). Theoretical X-ray solution scattering curves were calculated by CRYSOL (51) using atomic models of bent and extended conformations that included transmembrane domains (Supplemental Fig. 3A-C). These curves were processed by GNOM (41) to calculate distance distribution curves.

Supplemental Fig. 5. Least-square fitting of X-ray solution scattering curves. (A-C) Comparison of experimentally collected X-ray solution scattering curves (*black lines*) with calculated scattering curves derived from atomic models for (A) Ca^{2+}/Mg^{2+}, (B) Mn^{2+}/Ca^{2+}, and (C) Mn^{2+}/Ca^{2+} with L-739758 (*colored lines*). Theoretical X-ray solution scattering curves were calculated by CRYSOL (51) using atomic models of bent and extended conformations that included transmembrane domains (Supplemental Fig. 4A). (D) The percentage of each conformation is reported that gave the best least-square fit with each ensemble model, as shown in A-C. Least-square fitting to experimental data was performed in MATLAB (MathWorks, Natick, MA, USA).

Supplemental Fig. 6. Detergent stability screen. Whole blood-derived human platelets were solubilized in at least 3x CMC of various detergents and incubated for 1 hr at RT. $\alpha_{IIb}\beta_3$ was captured onto ELISA plate wells using AP3, an anti-β_3 antibody, and then incubated with biotinylated 7E3, an anti-β_3 antibody in TBS, pH 7.4 with 3x CMC of desired detergent. Amount of biotinylated 7E3 bound was quantitated by the addition of avidin peroxidase conjugate, color was developed using ABTS substrate and read in an Emax platereader (Molecular Devices, Sunnyvale, CA, USA). After 3 days at RT each sample was reassayed. Each sample was repeated two times.

A Ca^{2+}/Mg^{2+}

EM field views

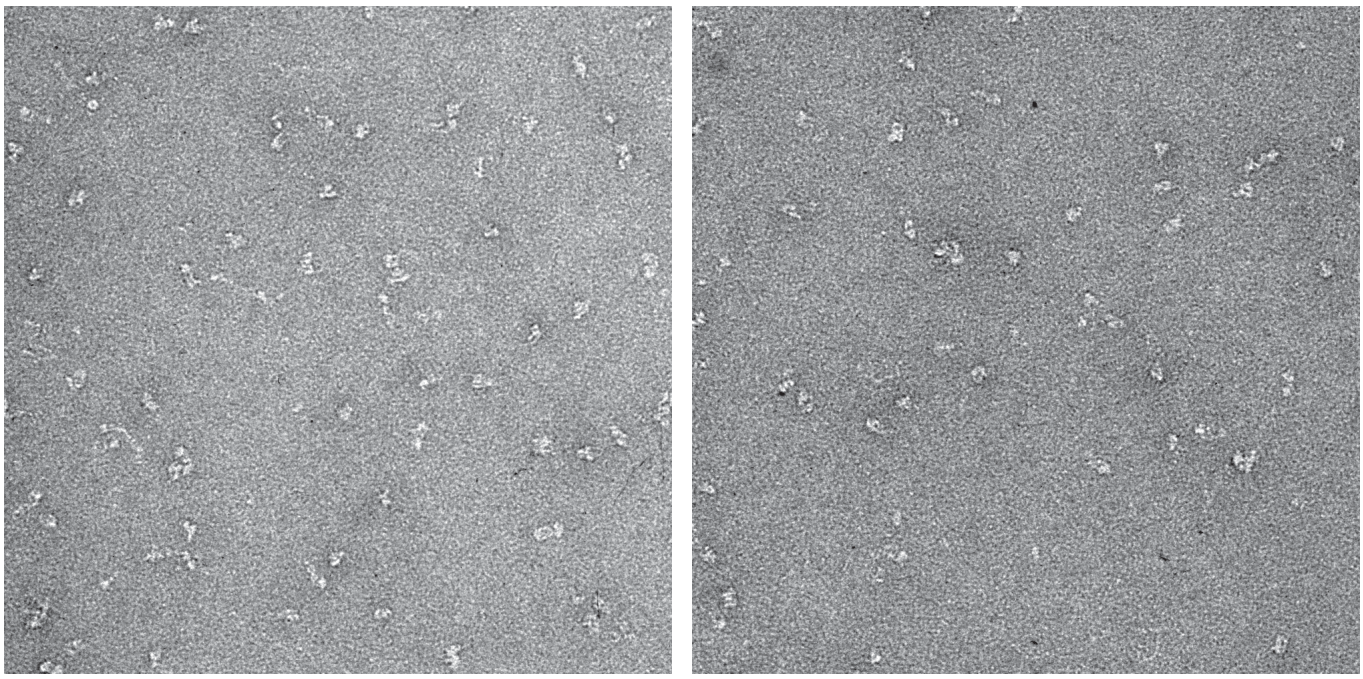

100 nm

2D class averages

7,213 particles 91% bent, 9% extended-closed

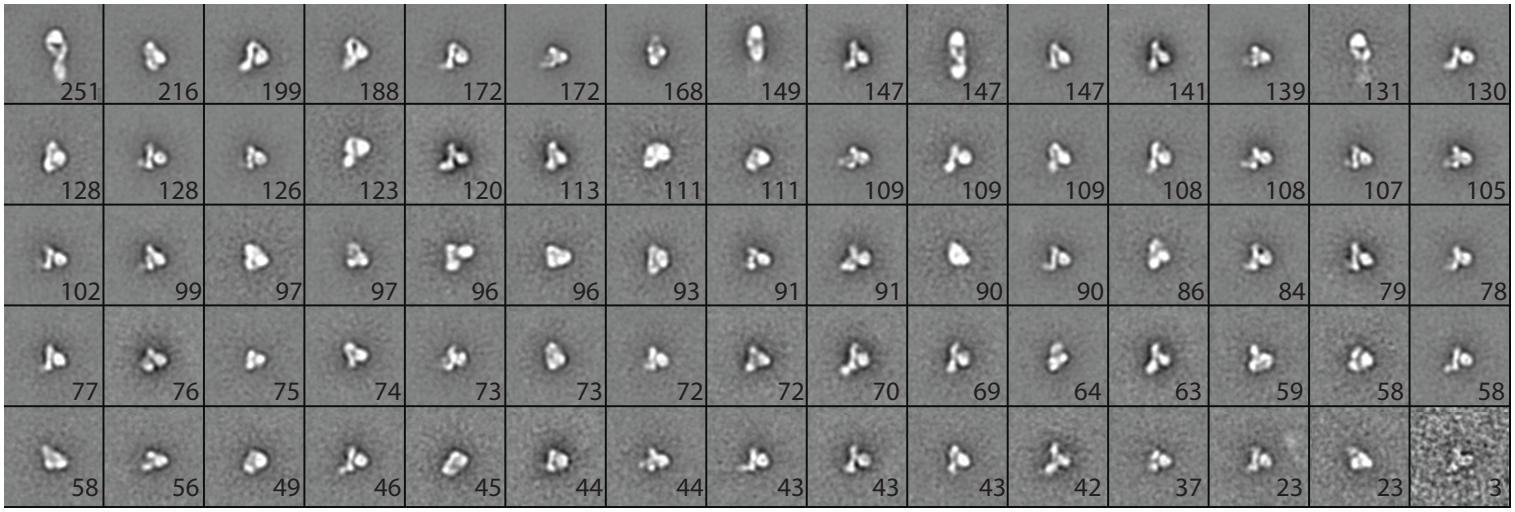

20 nm

75 classes

Supplemental Figure 1

B Mn^{2+}/Ca^{2+}

EM field views

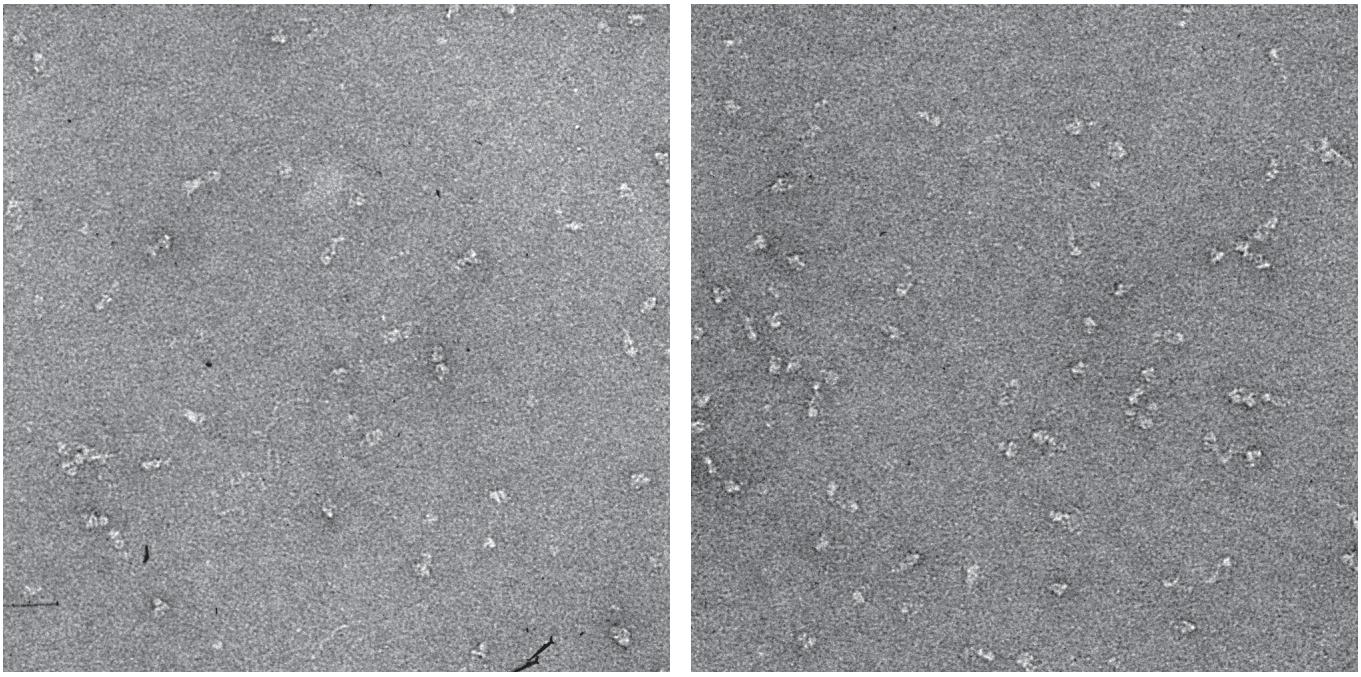

100 nm

2D class averages

12,145 particles 60% bent, 26% extended-closed, 14% extended-open

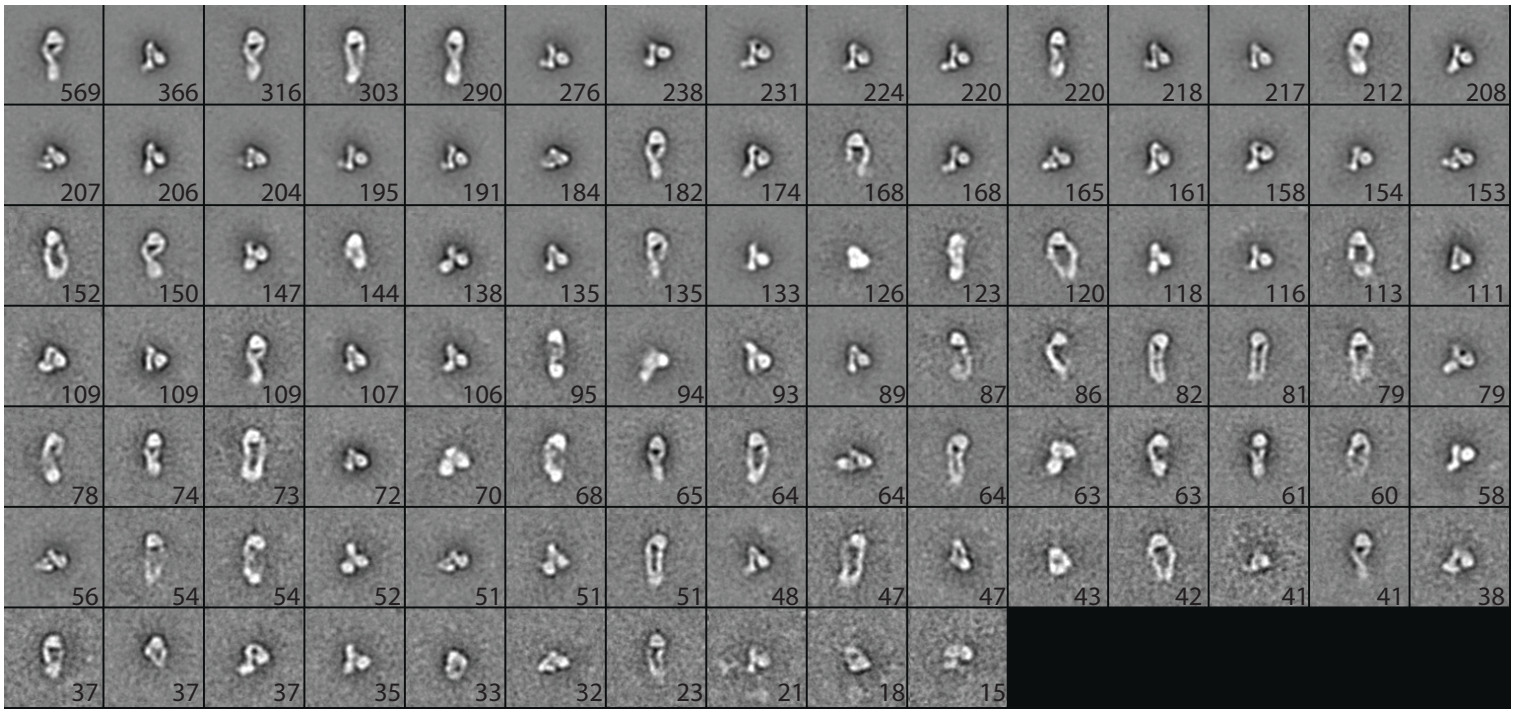

20 nm

100 classes

Supplemental Figure 1

C Mn^{2+}/Ca^{2+} + L-739758

EM field views

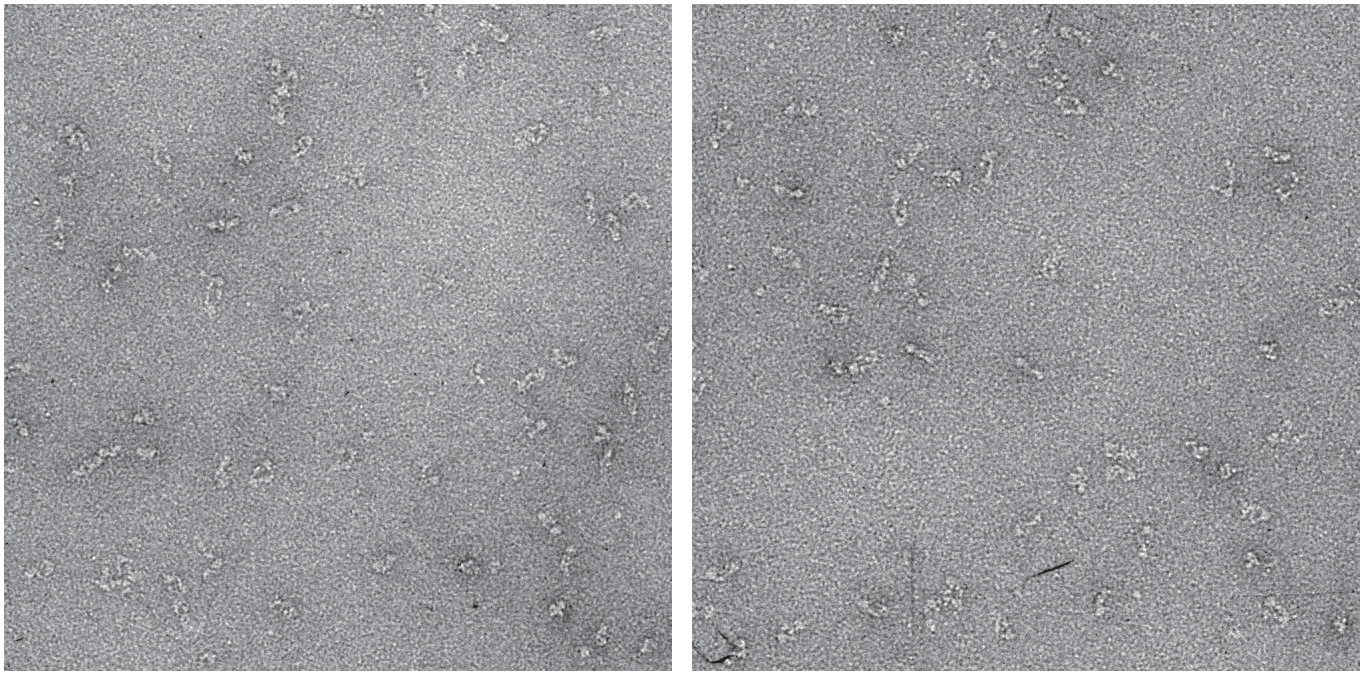

100 nm

2D class averages

10,934 particles 20% bent, 19% extended-closed, 61% extended-open

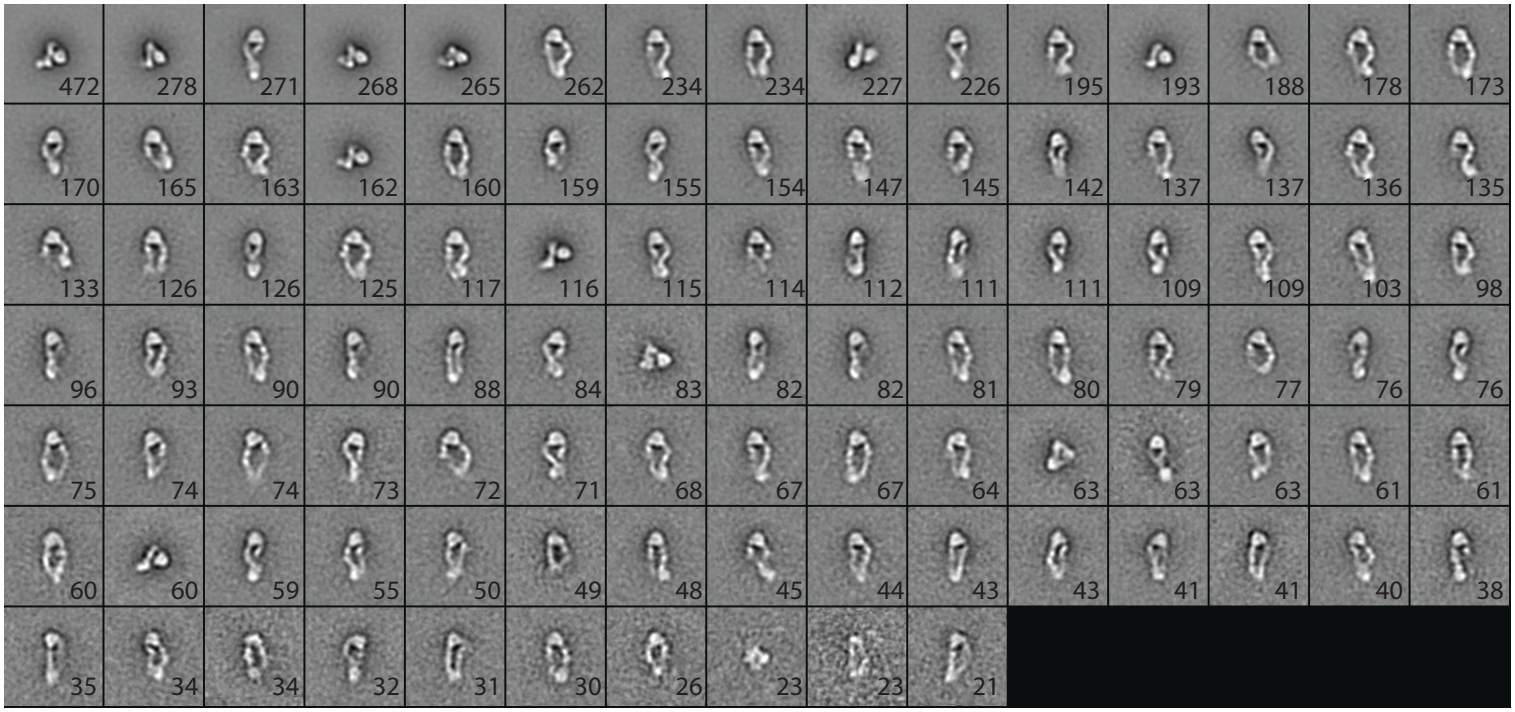

20 nm

100 classes

Supplemental Figure 1

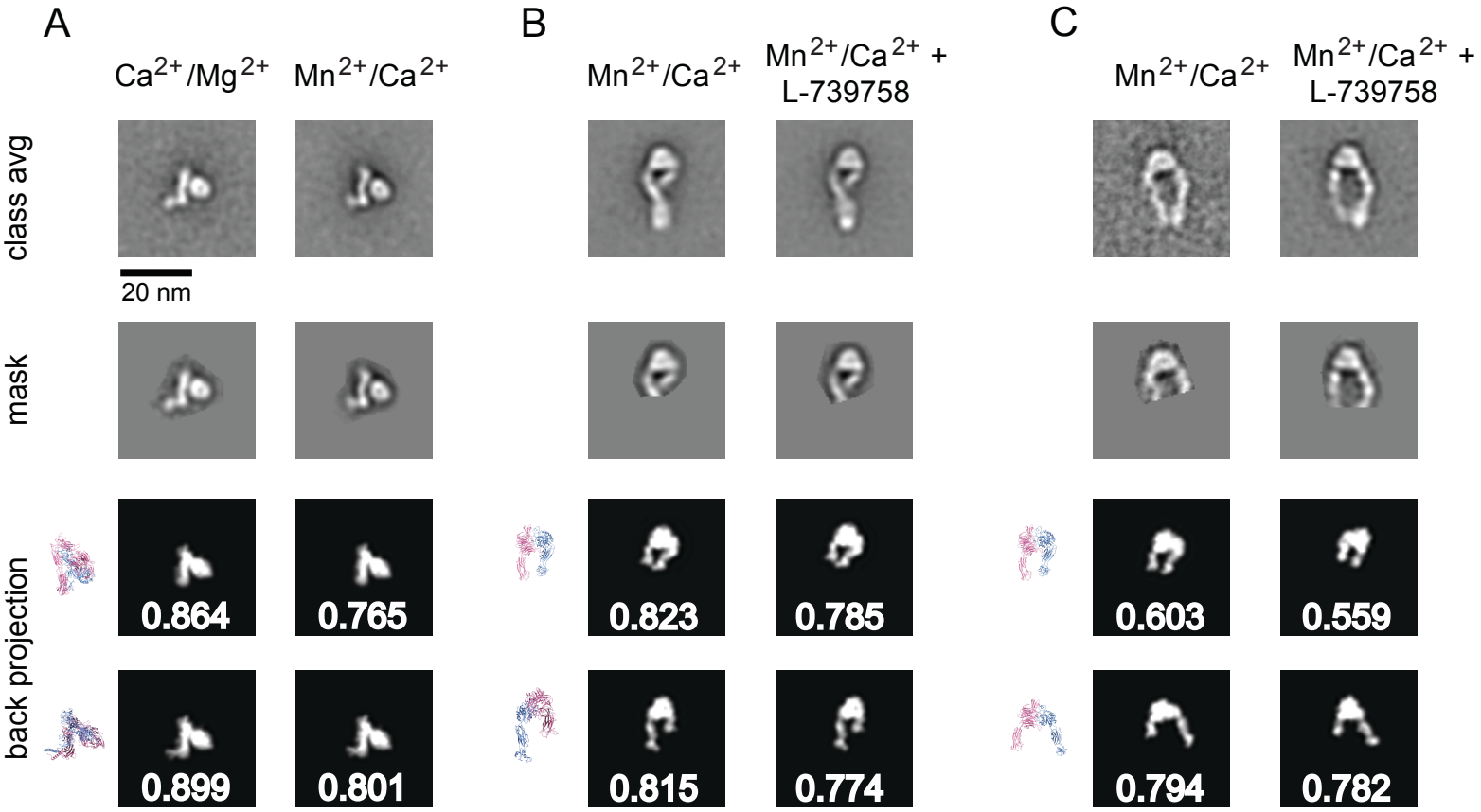

Supplemental Figure 2

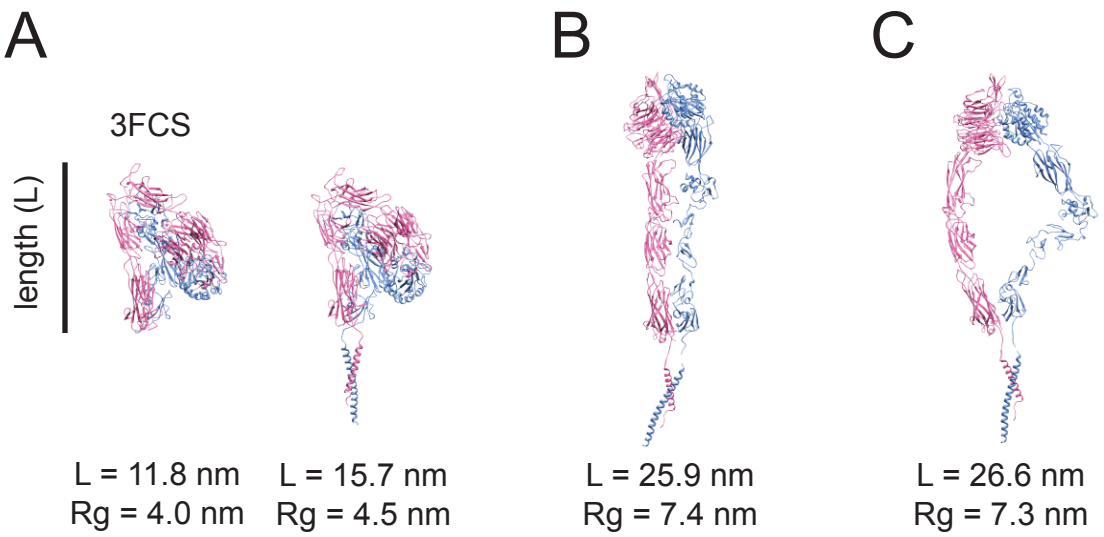

Supplemental Figure 3

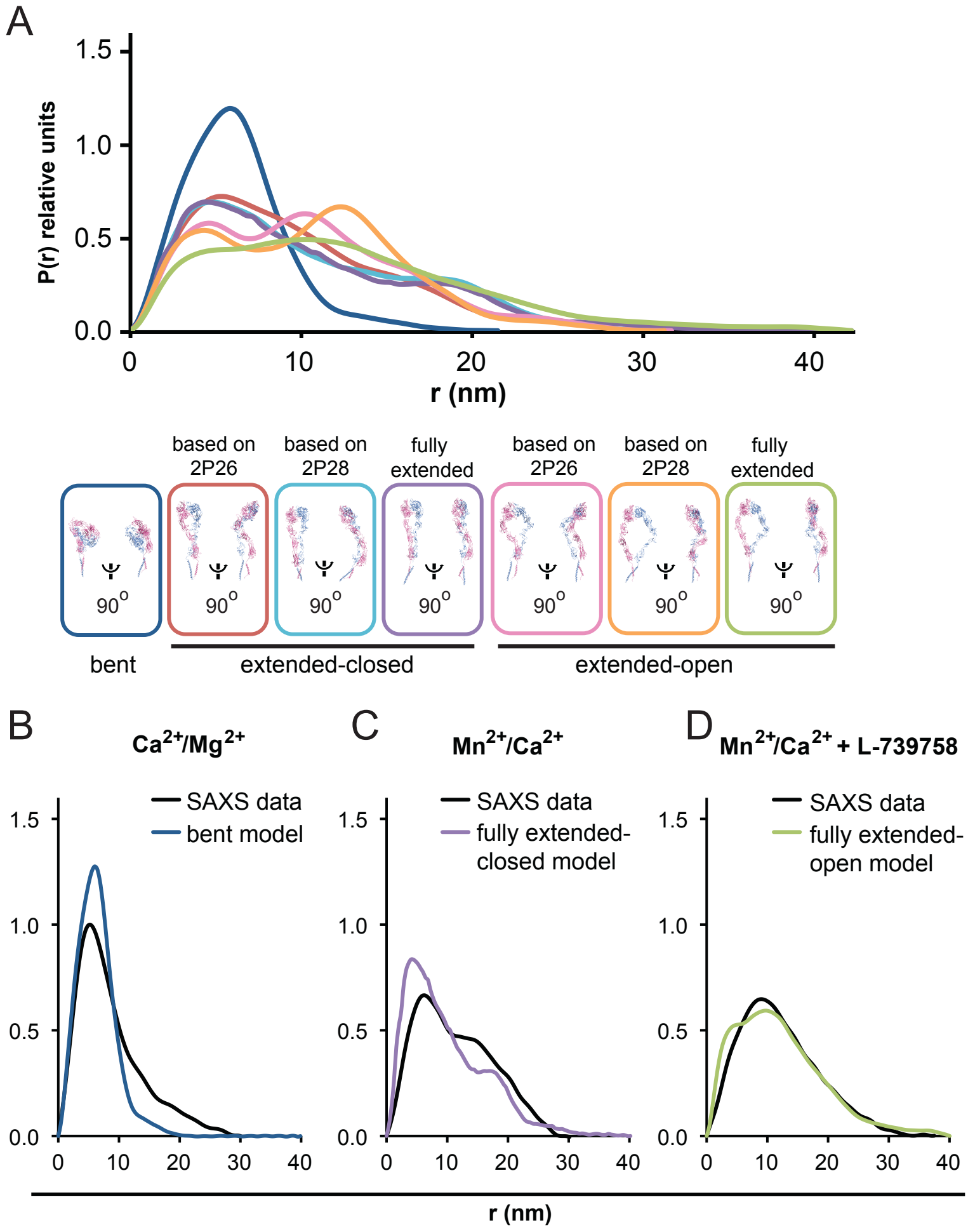

Supplemental Figure 4

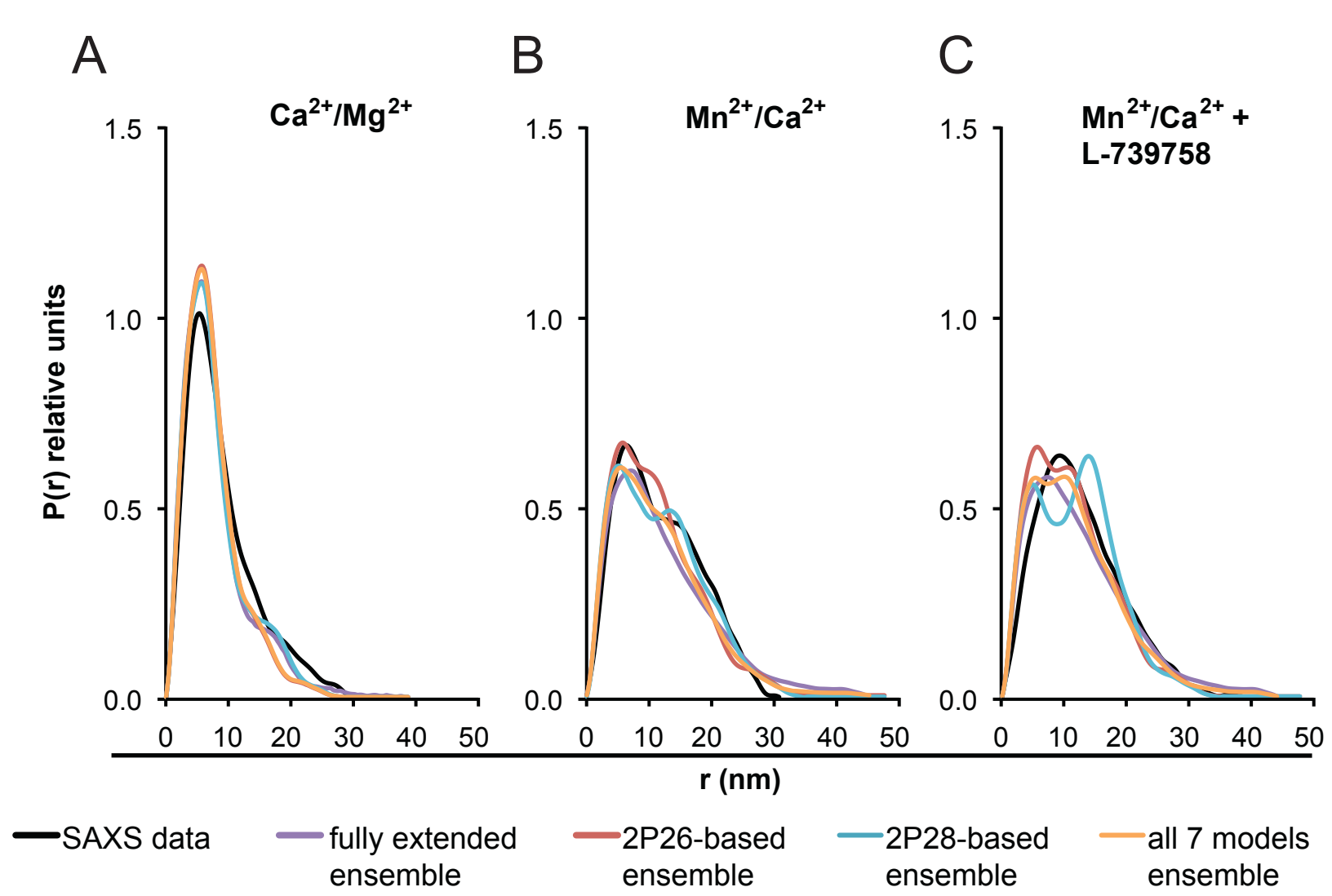

D

SAXS data	Ca^{2+} /Mg^{2+}	Mn^{2+}/Ca^{2+}	Mn^{2+}/Ca^{2+} + L-739758
fully extended ensemble	50% bent 50% extended-closed fully extended 0% extended-open fully extended	20% bent 5% extended-closed fully extended 75% extended-open fully extended	15% bent 0% extended-closed fully extended 85% extended-open fully extended
2P26-based ensemble	53% bent 43% extended-closed 2P26 based 4% extended-open 2P26 based	5% bent 53% extended-closed 2P26 based 42% extended-open 2P26 based	8% bent 27% extended-closed 2P26 based 65% extended-open 2P26 based
2P28-based ensemble	49% bent 51% extended-closed 2P28 based 0% extended-open 2P28 based	0% bent 53% extended-closed 2P28 based 47% extended-open 2P28 based	0% bent 11% extended-closed 2P28 based 89% extended-open 2P28 based
all 7 models ensemble	50% bent 50% extended-closed fully extended	8% bent 19% extended-closed 2P26 based 21% extended-closed 2P26 based 22% extended-open 2P28 based 30% extended-open fully extended	9% bent 39% extended-open 2P26 based 52% extended-open fully extended

Supplemental Figure 5

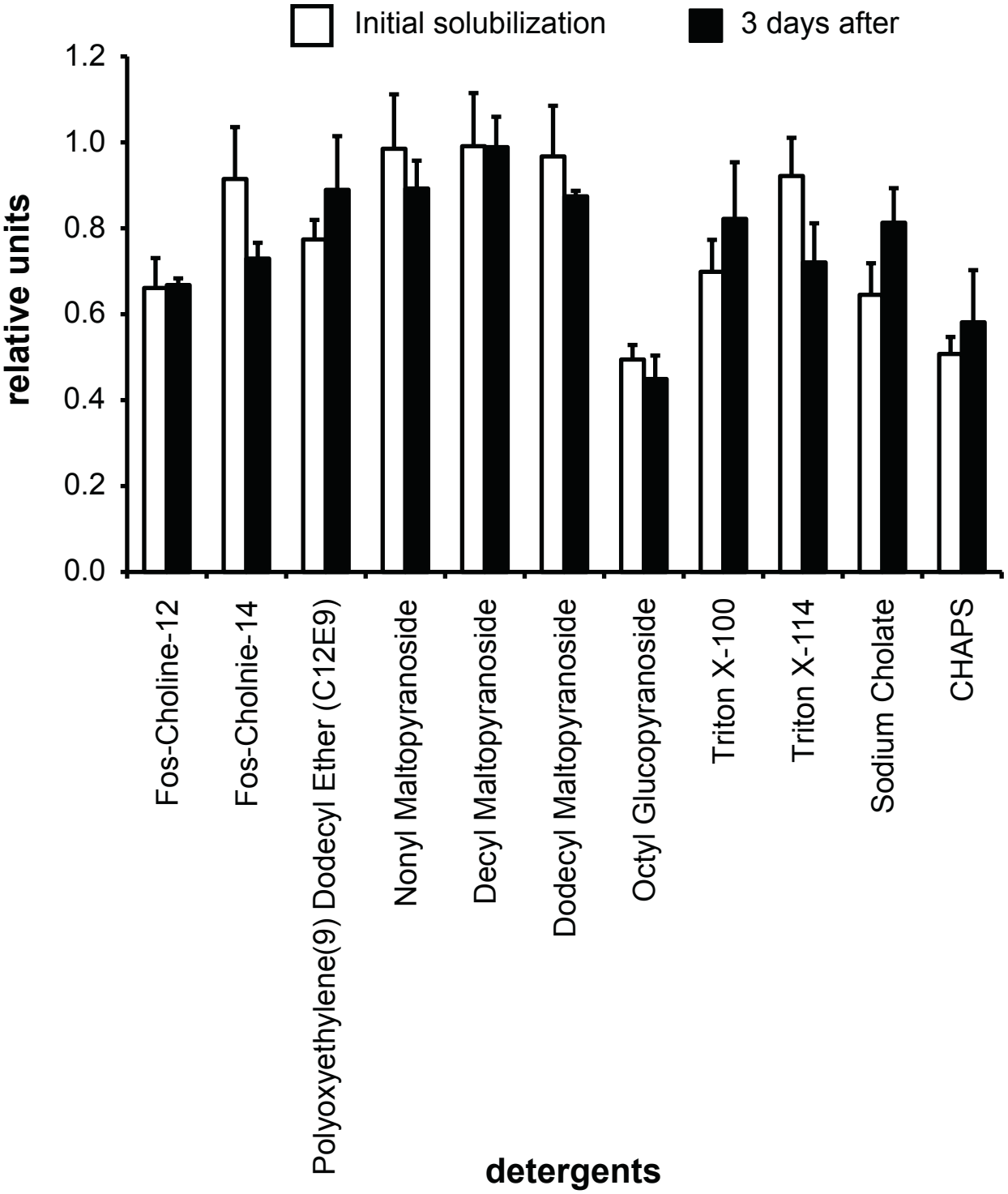

Supplemental Figure 6